International Journal of Computational Intelligence Systems (2022) 15:64
https://doi.org/10.1007/s44196-022-00119-z

RESEARCH ARTICLE

Absorption Chiller/Kalina Cycle Coupled System for Low-Grade Waste Heat Recovery in Hydrate-Based CO_2 Capture Process: An Economic and Exergetic Study

Zhiqiang Liu[1] · Kangrui Wang[1] · Nan Xie[1]

Received: 12 May 2022 / Accepted: 25 July 2022

Abstract

This study investigates a coupled system combined by a LiBr/H_2O absorption refrigeration cycle and a Kalina cycle, to recover waste heat from a hydrate-based CO_2 capture process. The optimal system operation has been obtained. Payback time, Return on investment, Net present value and Discounted cash flow rate of return are selected as the evaluation indicators for a comprehensive economic analysis. Cash flow patterns are obtained for different discounted interest rates and electricity prices. Exergy analysis is conducted and the exergy loss of each component is calculated. Results show that in comparison with the individual Kalina cycle, the net electricity generation is increased by around 45%. The highest thermal efficiency of this coupled system is 16.78%. Payment balance can be achieved with a payback time of 6 years. The purchase price of heat exchanger occupies the largest capital investment. Exergy efficiency of this system is obtained as 36.89%. Major system irreversibility occurs in heat transfer processes of heat exchangers and the largest exergy loss is found in generators of both subcycles. Reducing the heat transfer irreversibility and the size of heat exchangers are greatly encouraged in future efforts.

Keywords Economic analysis · Exergy analysis · LiBr/H_2O absorption chiller · Kalina cycle · Low-grade waste heat · CO_2 capture

Abbreviations

CEPCI	Chemical Engineering Plant Cost Index
COP	Coefficient of performance
CS	Carbon steel
DCFRR	Discounted cash flow rate of return
HT	High-temperature
KC	Kalina cycle
LBAC	LiBr/H_2O absorption chiller
LiBr	Lithium bromide
LMTD	Logarithmic mean temperature difference
LT	Low-temperature
NPV	Net present value
ROI	Return on investment
SS	Stainless steel
TBAB	Tetra-n-butylammonium bromide

✉ Nan Xie
xienan@csu.edu.cn

[1] School of Energy Science and Engineering, Central South University, Changsha 410083, People's Republic of China

1 Introduction

Kalina cycle (KC) is a promising approach of low- and medium-temperature waste heat utilization. Compared with the isothermal evaporation, the ammonia–water mixture of KC provides a better match to sensible heat sources. It is because the ammonia vaporizes at first when heated, the temperature and the solution concentration are both varying during the heat transfer process [1]. Low temperature heat of solar energy [2], cyclone preheater exhaust gases [3] and power plant exhaust gases [4] can be transformed into electricity using the Kalina cycle. This bottoming cycle has several types according to heat sources. Types of KCS-11 and KCS-34 are the most proper types for heat source temperature below 200 °C [5–7]. Absorption refrigeration system can also utilize the thermal energy from low temperature heat sources. In comparison with vapor compression system, absorption chiller has a low electricity consumption. It also requires low maintenance fees because of having no moving components [8] and causes less environmental pollution [9]. In the absorption chiller, working pairs such as ammonia/water and lithium bromide/water cause no global warming and ozone depletion effects. Absorption refrigeration cycle using ammonia/water is more complex because of the separate rectifier process [10]. Investigation on LiBr/H_2O absorption chiller (LBAC) has been extensively carried out, such as in low-concentrating photovoltaic modules [9], detergent production factory [11], low- and medium-temperature solar collectors [12] and even with multi-heat source waste heat [13].

Exergy analysis locates the position of exergy destruction and finds the causes for the process irreversibility. It is critical for both energy savings and resource conservations. A combined system of absorption–compression refrigeration was developed by Mohammadi and Ameri [14]. They used the absorption chiller to enhance the compression chiller and investigated the efficiency through the first and the second laws of thermodynamics. Irreversibility and exergy destruction in different components of a single-effect absorption/vapor compression-coupled system were calculated [15], the maximum exergy destruction was found in the condenser and generator. They also reported that the minimum system exergy destruction occurs at generator temperature of 60 °C. Eleven configurations of an LBAC/transcritical CO_2 compression-coupled system were designed and energy and exergy analysis were conducted individually [16]. Exergy analysis of a single effect LBAC with a flat-plate-collector array was conducted and the generator inlet temperature from 70 to 80 °C was recommended for achieving high exergetic efficiency [17]. Absorption chiller was integrated to make full use of the heat of the lean solution in a Kalina cycle before it enters the recuperator [18]. Results shown that the coupled system presents a higher exergy efficiency and more net power output than separate systems. Exergeoconomic analysis of an ammonia–water absorption refrigeration/KC-coupled cycle was carried out to investigate the effect of the ambient temperature on the exergy efficiency and total product unit cost [19]. Wang et al. [20] employed the turbine exhaust gas to achieve higher ammonia concentration and to produce cold output at the same time. Their exergy analysis results shown that the major exergy destruction is in the heat exchangers. Two absorption refrigeration/KC combined cycles were also studied by Shokati et al. [21, 22]. They pointed that the largest exergy losses were obtained in the boiler, absorber and rectifier. Besides, this double effect absorption refrigeration/KC has a higher thermal efficiency while a longer payback period. Energy, exergy and economic analysis was performed to investigate and to make comparison between the Kalina cooling-power cycle and Kalina LiBr–H_2O absorption chiller cycle systems [23, 24]. It was suggested to make system modifications to reduce the inefficiency in the absorber and heat exchangers. A hybrid system was developed using the low-grade heat from the solar cells [25]. This system generated electrical power with an exergy efficiency of 26.5%. The waste thermal energy was converted into cold energy production, which was employed to cool the turbine-outlet stream [26]. Compared with the individual Kalina cycle, the total electrical power production was enhanced because of higher expansion ratio of the turbine. In our previous effort, a LiBr/H_2O absorption refrigeration cycle and a Kalina cycle were integrated in cascade [27]. A detailed parametric analysis was carried out. However, this coupled system of LBAC and KC has never been investigated from the exergetic and economic aspects.

Hydrate-based CO_2 capture is a novel technology for CO_2 emission reduction which has a simple capture process and produces no by-product. However, this technology has a higher energy penalty than conventional CO_2 capture technologies [28]. Hydrate-based CO_2 capture is a technology of reducing CO_2 emission by forming CO_2 hydrate. While forming hydrate using the flue gases always requires higher pressure and lower temperature [29–31]. With the help of hydrate promoters, such as tetra-n-butylammonium bromide (TBAB), the formation condition would be greatly alleviated [32]. Flue gas is compressed to the equilibrium pressure and cooled to the equilibrium temperature at first. It then enters the formation unit to form hydrate with the additive solution. Forming CO_2 hydrate requires much lower pressure than forming N_2 hydrate at the same temperature, CO_2 would be captured in the hydrate slurry [33, 34]. The hydrate is introduced into the dissociation unit to release this acid gas through heating or depressurization [34, 35]. In this way, the gaseous carbon dioxide is concentrated. Kalina cycle and organic Rankine cycle were integrated with CO_2 capture by Pan et al. [36], they utilized the low-grade waste heat to achieve greenhouse gas emissions reduction. In this work, to reduce the energy penalty of hydrate-based CO_2 capture, this integrated system is employed to recover the waste heat from a two-stage hydrate-based CO_2 capture process. Employing the absorption chiller as an auxiliary cooling cycle for the power generation cycle, the wasted thermal energy is fully utilized in cascade. Economic analysis and exergy analysis are then carried out in this research for an in-depth understanding of this absorption chiller/Kalina cycle-coupled system. This research will also be useful for energy penalty reduction in the hydrate-based CO_2 capture process.

2 System Description

The coupled system consists of an absorption chiller using lithium bromide/water as the working pair and a Kalina cycle of type KCS-34. The integration is realized relying on the heat transfer process in an evaporator. The absorption refrigeration cycle is regarded as an auxiliary cooling cycle for the electrical power generation enhancement in the Kalina cycle. Both subcycles are driven by a given low temperature waste heat. This low temperature thermal energy contains two parts. The part with higher temperature Q_H is for electrical power generation in the Kalina cycle. The other part Q_L is for cooling output in the absorption chiller. The cooling output is to cool down the exhaust stream of the power generation cycle. Eventually, this specific thermal energy is fully recovered by the coupled system in a cascade process. The coupled system is illustrated in Fig. 1. In the absorption chiller, the absorbent is lithium bromide and the refrigerant is water. The lean solution absorbs the thermal energy Q_L in Generator 1 and turns into the refrigerant vapor and the strong solution. The former stream is cooled down in Condenser, throttles in Valve 1 and then flows into the cold side of the Evaporator to provide cold energy to the Kalina cycle. The strong solution releases heat in the Heat exchanger, throttles in Valve 2 and then enters the Absorber with the saturated vapor to become a lean solution. The lean solution is then pressurized in the Pump 1, recovers heat in the Heat exchanger and then goes into the generator for continuous cycle operation. In the Kalina cycle, the strong solution absorbs the thermal energy Q_H in Generator 2 and becomes an ammonia vapor and a dilute solution. The vapor expands in the Turbine for electricity production. The dilute solution discharges heat in the high-temperature recuperator (HT recuperator), throttles in Valve 3 and then mixes with the turbine exhaust gas in the Mixer to become a strong solution. This strong solution discharges heat in the low-temperature recuperator (LT recuperator) and is further cooled in the hot side of the Evaporator. It is pressurized in Pump 2, recovers heat in the low-temperature and high-temperature recuperators and then it enters the generator for continuous power generation.

3 Methodology

3.1 Basic Assumptions

Process simulation of this coupled system is developed in Aspen Plus software. ELECNRTL model is suitable for various electrolyte solutions in medium pressure systems hence it is selected for the absorption chiller. PSRK model is chosen for the Kalina cycle, because it runs at relatively high pressure [37]. Electrolyte properties for the $LiBr/H_2O$ absorption chiller and the binary parameters for the Kalina cycle have been obtained in our previous research [38, 39]. Detailed block type and parameter specification are given

Fig. 1 Schematic diagram of the coupled system

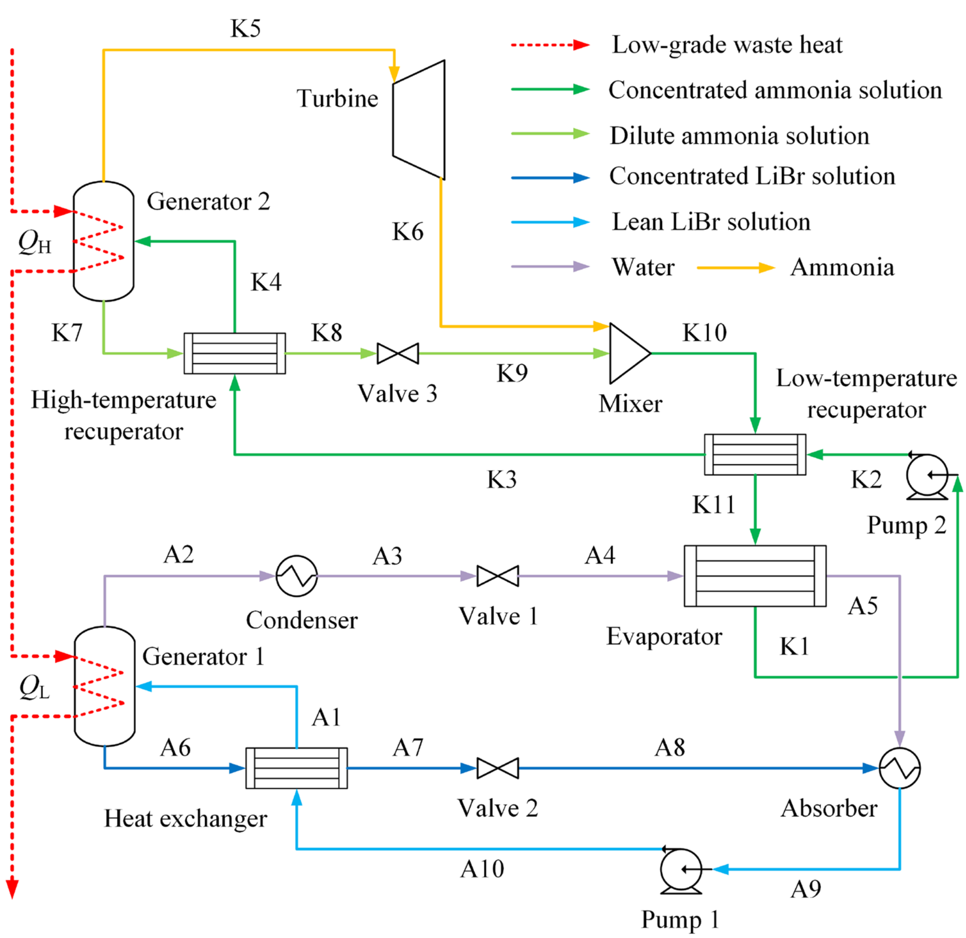

in Table 1. Generators in both subcycles are replaced by a Heater model as well as a Flash2 model. The binary solutions absorb heat in the Heater models. The vapor streams are separated in the Flash2 models. To guarantee the accuracy and correctness of these simulated results, the LiBr/H_2O absorption refrigeration cycle has been validated previously [37]. The simulated results of the Kalina cycle is also compared with the published literature [26] and good agreement has been obtained [27].

A low temperature waste heat is specified in present research with a temperature ranging from 90 to 150 °C. It has. This given waste heat can be divided into two parts using a certain segment temperature. The segment temperature is determined when the absorption chiller fully covers the cooling demand in the Kalina cycle. In addition, this temperature has to make sure that the given waste heat is fully recovered in this cascade process. Thus, there is only one segment temperature for each operation status. The low-temperature part is unsuitable for electricity generation hence it is utilized for cooling output from the absorption chiller. The segment temperature determines the generator temperature of the Kalina cycle (considering the minimum temperature approach is 10 °C). The generator temperature of the absorption chiller is 80 °C (considering a temperature decrease of 10 °C from the lower temperature limit 90 °C). Refrigeration temperatures of 2, 3, 5, 7 and 10 °C are assumed for the cooling output from the absorption chiller. The temperature of cooling water in present work is consistent with the ambient temperature of 30 °C. Considering the minimum temperature approach of 5 °C, the absorber temperature and condenser temperature are assumed to be 35 °C. Based on the literature review, some reasonable assumptions are currently made: (1) The whole process is at steady state [18–20, 24, 40]; (2) Changes in the kinetic and potential energy are thought as negligible [18, 19, 40]; (3) Heat discharged to environment as well as pressure drop in the devices and pipes are neglected [5, 18–20, 24, 40]; (4) Ammonia solution at the generator inlet/absorber outlet is saturated liquid and the ammonia at the generator outlet/absorber inlet is saturated vapor [18–20, 24, 40]; (5) LiBr/H_2O solution at the generator/absorber outlet is saturated liquid and the refrigerant at the condenser inlet and the evaporator outlet is saturated vapor [24]; (6) Isentropic efficiencies are specified for the turbine and the pumps [19, 20]; (7) Leakage of working fluids is assumed to be negligible [18]; (8) All the throttling processes are thought as isenthalpic [18, 20, 40]; (9) Ammonia concentration of Kalina cycle is specified as 0.7 (mass based) [1, 18, 26, 41].

3.2 Mathematical Model

On the basis of the energy balance and mass balance algorithms, the mathematical models of this integrated system have been established in this section. Calculation and evaluation of individual device and each stream are hence carried out. The calculation equations of each device are given as

(1) LiBr/H_2O absorption chiller:

Generator 1:

Table 1 Block type and specification

Block name	Type	Specification
LiBr/H_2O absorption refrigeration cycle		
Generator 1	Heater Flash2	Inlet heat stream, specified; Pressure drop, 0 kPa Duty, 0 kW; Pressure drop, 0 kPa
Condenser	Heater	Vapor fraction, 0; Pressure drop, 0 kPa
Valve 1	Valve	Outlet pressure, specified
Evaporator (cold side)	Heater	Vapor fraction, 1; Pressure drop, 0 kPa
Absorber	Heater	Vapor fraction, 0; Pressure drop, 0 kPa
Heat exchanger	HeatX	Hot outlet-cold inlet temperature approach, 5 °C
Valve 2	Valve	Outlet pressure, specified
Pump 1	Pump	Discharge pressure, specified; Efficiency, 0.90
Kalina cycle		
Generator 2	Heater Flash2	Temperature, specified; Pressure drop, 0 kPa Duty, 0 kW; Pressure drop, 0 kPa
Turbine	Turbine	Isentropic; Discharge pressure, specified; Isentropic efficiency, 0.88
Mixer	Mixer	Pressure drop, 0 kPa
High-temperature recuperator	HeatX	Hot outlet-cold inlet temperature approach, 5 °C
Valve 3	Valve	Outlet pressure, specified
Low-temperature recuperator	HeatX	Hot inlet-cold outlet temperature approach, 5 °C
Evaporator (hot side)	Heater	Temperature, specified; Pressure drop, 0 kPa
Pump 2	Pump	Discharge pressure, specified; Efficiency, 0.90

$$m_{A1} = m_{A2} + m_{A6} \tag{1}$$

$$m_{A1}h_{A1} + Q_L = m_{A2}h_{A2} + m_{A6}h_{A6} \tag{2}$$

$$m_{A1}x_{A1} = m_{A6}x_{A6} \tag{3}$$

where the subscripts A1, A2 and A6 refer to streams in the absorption refrigeration cycle; m is the mass flow rate; h is the specific enthalpy; Q_L is the thermal energy enters the Generator 1; x is the LiBr concentration of streams.

Condenser:

$$m_{A2} = m_{A3} \tag{4}$$

$$Q_{condenser} = m_{A2}h_{A2} - m_{A3}h_{A3} \tag{5}$$

where $Q_{condenser}$ is the thermal energy removed out of the system from the condenser.

Valve 1:

$$m_{A3} = m_{A4} \tag{6}$$

$$m_{A3}h_{A3} = m_{A4}h_{A4} \tag{7}$$

Evaporator (cold side):

$$m_{A4} = m_{A5} \tag{8}$$

$$Q_0 = \left| m_{A4}h_{A4} - m_{A5}h_{A5} \right| \tag{9}$$

where Q_0 is the cooling capacity output from the LiBr/H_2O absorption chiller.

Heat exchanger:

$$m_{A6} = m_{A7} \tag{10}$$

$$m_{A6}h_{A6} - m_{A7}h_{A7} = m_{A1}h_{A1} - m_{A10}h_{A10} \tag{11}$$

$$m_{A6}x_{A6} = m_{A7}x_{A7} \tag{12}$$

$$m_{A10} = m_{A1} \tag{13}$$

$$m_{A10}x_{A10} = m_{A1}x_{A1} \tag{14}$$

Valve 2:

$$m_{A7} = m_{A8} \tag{15}$$

$$m_{A7}h_{A7} = m_{A8}h_{A8} \tag{16}$$

$$m_{A7}x_{A7} = m_{A8}x_{A8} \tag{17}$$

Absorber:

$$m_{A5} + m_{A8} = m_{A9} \tag{18}$$

$$m_{A5}h_{A5} + m_{A8}h_{A8} = m_{A9}h_{A9} + Q_a \tag{19}$$

$$m_{A8}x_{A8} = m_{A9}x_{A9} \tag{20}$$

where Q_a is the thermal energy taken away from the Absorber.

Pump 1:

$$m_{A9} = m_{A10} \tag{21}$$

$$m_{A9}x_{A9} = m_{A10}x_{A10} \tag{22}$$

$$W_{pump\ 1} = \frac{1}{\eta_p} m_{A9}(h_{A10} - h_{A9}) \tag{23}$$

where $W_{pump\ 1}$ is the electrical power consumption of Pump 1; η_p is the overall efficiency.

(2) Kalina cycle:

Generator 2:

$$m_{K4} = m_{K5} + m_{K7} \tag{24}$$

$$m_{K4}h_{K4} + Q_H = m_{K5}h_{K5} + m_{K7}h_{K7} \tag{25}$$

$$m_{K4}x_{K4} = m_{K5}x_{K5} + m_{K7}x_{K7} \tag{26}$$

where the subscripts K4, K5 and K7 refer to streams in the Kalina cycle; Q_H is the thermal energy into the Generator 2; x is the ammonia concentration of the streams.

Turbine:

$$m_{K5} = m_{K6} \tag{27}$$

$$W_{turbine} = m_{K5}(h_{K5} - h_{K6}) \times \eta_t \tag{28}$$

$$m_{K5}x_{K5} = m_{K6}x_{K6} \tag{29}$$

where $W_{turbine}$ is the electricity output from the Turbine by an expansion process; η_t is the efficiency of the turbine.

High-temperature recuperator:

$$m_{K7} = m_{K8} \tag{30}$$

$$m_{K7}h_{K7} - m_{K8}h_{K8} = m_{K4}h_{K4} - m_{K3}h_{K3} \tag{31}$$

$$m_{K7}x_{K7} = m_{K8}x_{K8} \tag{32}$$

$$m_{K3} = m_{K4} \tag{33}$$

$$m_{K3}x_{K3} = m_{K4}x_{K4} \tag{34}$$

Valve 3:

$$m_{K8} = m_{K9} \tag{35}$$

$$m_{K8}h_{K8} = m_{K9}h_{K9} \tag{36}$$

$$m_{K8}x_{K8} = m_{K9}x_{K9} \tag{37}$$

Mixer:

$$m_{K6} + m_{K9} = m_{K10} \tag{38}$$

$$m_{K6}h_{K6} + m_{K9}h_{K9} = m_{K10}h_{K10} \tag{39}$$

$$m_{K6}x_{K6} + m_{K9}x_{K9} = m_{K10}x_{K10} \tag{40}$$

Low-temperature recuperator:

$$m_{K10} = m_{K11} \tag{41}$$

$$m_{K10}h_{K10} - m_{K11}h_{K11} = m_{K3}h_{K3} - m_{K2}h_{K2} \tag{42}$$

$$m_{K10}x_{K10} = m_{K11}x_{K11} \tag{43}$$

$$m_{K2} = m_{K3} \tag{44}$$

$$m_{K2}x_{K2} = m_{K3}x_{K3} \tag{45}$$

Evaporator (hot side):

$$m_{K11} = m_{K1} \tag{46}$$

$$Q_0{}' = \left| m_{K11}h_{K11} - m_{K1}h_{K1} \right| \tag{47}$$

where $Q_0{}'$ is the heat discharged from the Kalina cycle.

Pump 2:

$$m_{K1} = m_{K2} \tag{48}$$

$$m_{K1}x_{K1} = m_{K2}x_{K2} \tag{49}$$

$$W_{\text{pump 2}} = \frac{1}{\eta_p} m_{K1}(h_{K2} - h_{K1}) \tag{50}$$

(3) Coefficient of performance (COP):

$$Q = Q_H + Q_L \tag{51}$$

$$Q_H = \frac{150 - T}{150 - 90} \times Q \tag{52}$$

where T is the segment temperature.

$$COP = \frac{Q_0}{Q_L} \tag{53}$$

$$\eta = \frac{\mathrm{W}_{\text{turbine}} - \mathrm{W}_{\text{pump 2}}}{\mathrm{Q}_{\mathrm{H}}} \tag{54}$$

where COP is the coefficient of performance of the LiBr/H_2O absorption chiller; η is the thermal efficiency of the Kalina cycle.

(4) Exergy analysis

Exergy analysis provides guidelines for achieving better process integration, which can save both primary energy and raw materials. It explains what makes a process inefficient and also quantifies the irreversibility of this process. The exergy in a stream is a combination of physical exergy, chemical exergy and mixing exergy. Physical exergy is the amount of work arising when reversibly changing a stream of pure component from a certain process status (T, P) to the reference state (T_0, P_0):

$$Ex_{\text{phy}} = -(H_i - H_i^0) + T_0(S_i - S_i^0) \tag{55}$$

where i refers to component i; H_i^0 and S_i^0 are the enthalpy and entropy of component i at reference state (T_0, P_0); H_i and S_i are the enthalpy and entropy of component i at a certain process status. The physical exergy presents the change of state without considering the mixing effects. The chemical exergy can be calculated as follows:

$$Ex_{\text{chem}} = \sum_i x_i Ex_{0,i} + \int RT_0 \sum_i x_i \ln x_i \tag{56}$$

where x_i represents the mole fraction of component i; $Ex_{0,i}$ is the standard chemical exergy of component i; R represents the universal gas constant.

Mixing has a negative effect on the work potential, because unmixing the components in a stream consumes work. The mixing exergy is the work arising when streams of pure components are mixed at process conditions (T, P):

$$Ex_{\text{mix}} = (H - \sum_i x_i H_i) - T_0(S - \sum_i x_i S_i) \tag{57}$$

where H and S are the enthalpy and entropy of a stream at a certain status. Exergy of this stream is given as

$$Ex = Ex_{\text{phy}} + Ex_{\text{chem}} + Ex_{\text{mix}} \tag{58}$$

Exergy efficiency is the second law efficiency of a certain system or process. It is a major criterion to evaluate the irreversibility of this system or process. Exergy efficiency can be calculated by

$$\eta_{ex} = \frac{Ex_{\text{total}} - Ex_{\text{loss}}}{Ex_{\text{total}}} = \frac{W}{Ex_{\text{total}}} \tag{59}$$

where η_{ex} is the exergy efficiency; Ex_{total} is the total exergy input in a process; Ex_{loss} means the exergy loss during a process; W is the work produced in this process.

4 Results and Discussion

4.1 Energy Efficiency Analysis

The segment temperature determines the generator temperature of the Kalina cycle. Higher generator temperature might lead to a better process performance. However, the higher the segment temperature is, the less thermal energy enters this cycle. The cold energy output increases with higher refrigeration temperature, while the electrical power generation decreases with the increase of refrigeration temperature. The best performance of the absorption chiller is obtained at refrigeration temperature of 10 °C, while that of the Kalina cycle is obtained at refrigeration temperature of 2 °C. The thermal energy Q_L into the absorption chiller is the waste heat from the Kalina cycle. It drives the auxiliary cycle to enhance the power generation cycle. For this reason, thermal efficiency of the Kalina cycle is the major criteria of this coupled system. The highest thermal efficiency of 16.78% is obtained at refrigeration temperature of 2 °C, turbine-inlet pressure of 3200 kPa and turbine-outlet pressure of 293 kPa. Thus, these are the optimal operation condition of this coupled system. This coupled system is also compared with an individual Kalina cycle at the same condition. After the integration, the working medium at the turbine outlet is further cooled to a lower temperature of 7 °C. It allows a lower discharge pressure from 768 to 293 kPa. The turbine expansion ratio increases, because the inlet pressure is the same. As a result, more electricity generation is obtained and the net output increases from 35.36 to 51.24 kW with an enhancement of 45%.

In the hydrate-based CO_2 capture process, compressing the flue gases to the hydrate equilibrium pressure leads to a significant temperature rise. Thus, the pressurized stream needs to be cooled down by cooling water and a huge amount of sensible heat would be wasted if the thermal energy is not recovered at all. It is necessary to make efforts to recover this wasted thermal energy by employing the coupled system mentioned above. A two-stage hydrate-based CO_2 separation process in pilot-scale was developed to improve the CO_2 concentration from 17 to 90% [42]. In this section, the flue gas is assumed to have a composition of 17% CO_2/83% N_2 from a coal-fired power plant. It has a temperature of 323 K and a pressure of 0.1 MPa. The hydrate formation condition of the first stage is assumed as 282 K and 3 MPa, while the corresponding value is 282 K and 2.5 MPa for the second stage [43]. During each hydrate dissociation process, the pressure loss is typically around 10^5 Pa hence it can be assumed as 0.5 MPa based on this research. Accordingly, the molar concentration of 0.29% is adopted as the appropriate TBAB concentration for post-combustion CO_2 capture in this work [44]. The formation enthalpy of CO_2-TBAB hydrate was measured as 313.2 kJ/kg (hydrate) (around 139 kJ/mol CO_2) [45]. Split fractions for CO_2 and N_2, the selectivity towards these gaseous substances during hydrate formation [46], are assumed to be 0.53 and 0.10, respectively [32, 47].

Simulated results of this capture process are illustrated in Fig. 2, including the temperature, pressure and mass flow rate of the main streams. Detailed block types and parameters specification are given in Table 2. The capture process operates in a pressure range from 1.9 to 3 MPa, being much higher than the possible pressure loss in each component and pipes. Thus, the pressure drop is also thought as negligible in this capture process. It can be easily noticed in Fig. 2 that the temperature of the gaseous stream emitted from the Compressor 1 is very high. In addition, the compression process in this compressor is actually a multi-stage

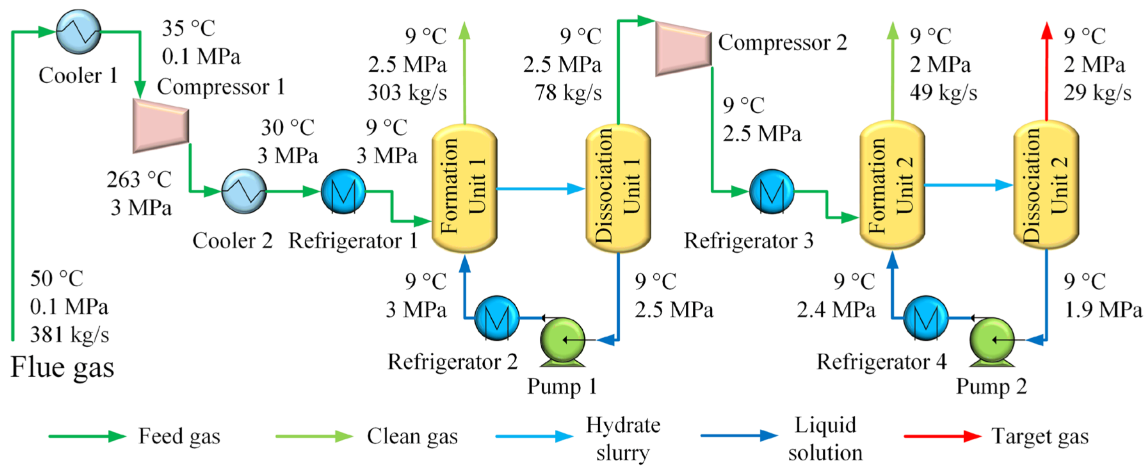

Fig. 2 Simulated results of the two-stage hydrate-based CO_2 capture

Table 2 Block types and parameters specification

Block name	Type	Specification
Cooler 1	Cooler	Pressure drop, 0 MPa; Temperature drop, −15 K
Compressor 1	Compressor	Centrifugal; Discharge pressure, 3 MPa; Adiabatic efficiency, 80%
Cooler 2	Cooler	Pressure drop, 0 MPa; Outlet temperature, 303 K
Refrigerator 1	Cooler	Pressure drop, 0 MPa; Outlet temperature, 282 K; $COP_1 = 3$
Formation/Dissociation Unit 1	Component Splitter	Overhead/bottoms split fractions 0.53/0.10; Pressure drop, 0.5 MPa
Pump 1	Pump	Discharge pressure, 3 MPa; Adiabatic efficiency, 80%
Refrigerator 2	Cooler	Pressure drop, 0 MPa; Outlet temperature, 282 K; $COP_2 = 3$
Compressor 2	Compressor	Centrifugal; Discharge pressure, 2.5 MPa; Adiabatic efficiency, 80%
Refrigerator 3	Cooler	Pressure drop, 0 MPa; Outlet temperature, 282 K; $COP_3 = 3$
Formation/Dissociation Unit 2	Component Splitter	Overhead/bottoms split fractions 0.53/0.10 Pressure drop, 0.5 MPa
Pump 2	Pump	Discharge pressure, 2.5 MPa; Adiabatic efficiency, 80%
Refrigerator 4	Cooler	Pressure drop, 0 MPa; Outlet temperature, 282 K; $COP_4 = 3$

compression with intercooling. Considering the mass flow rate of the pressurized flue gas being very large, the thermal energy containing in this pressurized stream would be huge. This part of energy would be totally wasted with the cooling water if no waste heat recovery action is taken. Therefore, it is worth to recover this wasted thermal energy by utilizing the aforementioned coupled system.

Figure 3 shows the schematic diagram of this waste heat recovery process. The waste heat with temperature lower than 150 °C is not easy to be re-utilized in many recovery efforts. This integrated system works efficiently in the temperature range from 90 to 150 °C. Thus, only the waste heat in this temperature range is in current consideration. The wasted thermal energy contains two parts: the high-temperature part and the low-temperature part. The Kalina cycle takes in the higher temperature part to realize electrical power generation. The latter one is for cold energy production in the absorption chiller. Thus, this given waste heat is fully used through the cascade utilization process. Thus, only this part of wasted thermal energy will be recovered in cascade in this research. The net power output is obtained as 4065 kW in the process simulation and this value is used in the following economic analysis.

4.2 Economic Analysis

Process economics is a critical part in the process design and it includes several major roles, such as evaluation of design options, process optimization and overall project profitability [48]. Therefore, economic analysis of the waste heat recovery process from the CO_2 hydrate-based capture system is absolutely necessary in this work. The economic analysis is conducted according to the procedure, e.g., Eqs. (60)–(64), described in the book of Robin Smith [48]:

$$C_{\mathrm{E}}^{0} = C_{\mathrm{B}}\left(\frac{Q}{Q_{\mathrm{B}}}\right)^{M} \tag{60}$$

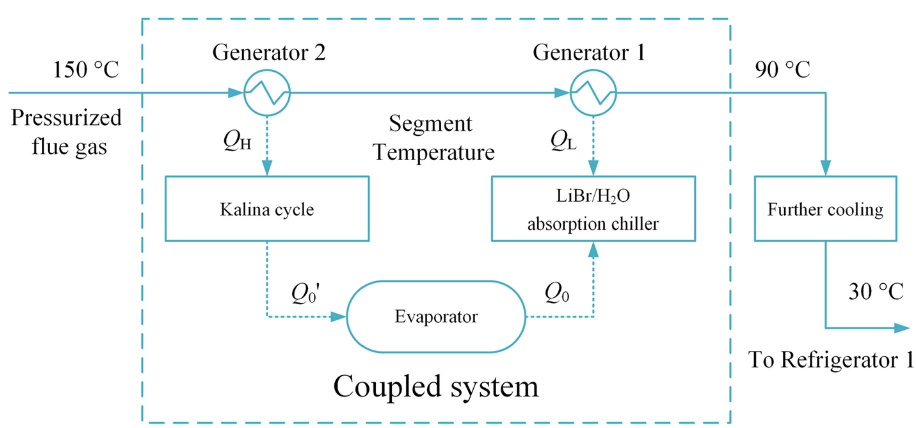

Fig. 3 Schematic diagram of the waste heat recovery process

where Q_B is the base size of an equipment and C_B is the base cost for this equipment with capacity Q_B; Q is the actual size of the equipment and C_E^{0} is the cost for this equipment with capacity Q; M is the cost exponent index depending on different equipment types:

$$C_E = C_B\left(\frac{Q}{Q_B}\right)^{M} f_M f_P f_T \tag{61}$$

where f_M is the correction factor for construction material of an equipment; f_P is the correction factor for design pressure of this equipment; f_T is the correction factor for design temperature; C_E is the actual cost for this equipment. Cost index should be employed in this economic analysis to keep the equipment price up to date:

$$\frac{C_{E,2000}}{C_{E,2019}} = \frac{INDEX_{2000}}{INDEX_{2019}} \tag{62}$$

where INDEX_{2000} is the cost index in year 2000; INDEX_{2019} is the cost index in year 2019; $C_{E,\,2000}$ is the equipment price in 2000; $C_{E,\,2019}$ is thought as the latest price for this equipment in 2019. The cost index adopted in present work is Chemical Engineering Plant Cost Index (CEPCI), a widely used resource for plant construction costs. The $CEPCI_{2000}$ is 394.1 and $CEPCI_{2019}$ is 607.5 (CEPCI of 2020 is not available yet) [49]. According to the reference [48], the purchase prices (delivered prices) of all the devices in the proposed system are estimated and calculated. The proposed system contains corrosive fluids (ammonia vapor, ammonia solution and LiBr solution) and operates at high pressure condition. For this reason, stainless steel is selected as the construction material for all the equipment except for the condenser. The inflow fluid (A2 in Fig. 1) and outflow fluid (A3) of this condenser are both pure H_2O. Hence, carbon steel is selected as the construction material of Condenser for the cost-effectiveness of this proposed system. Table 3 lists the purchase price of each equipment in this coupled system. The total purchase cost of these devices is calculated as \$ 7.54×10^{6} (U.S. dollar). It can be noticed that the purchase cost for heat exchanger occupies the largest portion (more than 50%) of the total cost. The gas turbine is the most expensive equipment in the whole system. However, it should be mentioned that the price information of turbine is not provided in this reference so the price of compressor is adopted for the cost estimation for gas turbine. In the work of Turton et al. [50], the price calculation of turbine is recommended to use the correlation equation: $\log_{10}C_E^{0} = 2.7051 + 1.4398\times\log_{10}(W_{\mathrm{turbine}}) - 0.1776\times[\log_{10}(W_{\mathrm{turbine}})]^2$ (where W_{turbine} is the work output of turbine). For comparison and validation, the same correction factors and cost index are employed. The calculated value $C_{E,\,2019}$ of turbine is obtained as \$ 2.15×10^{6},

Table 3 Equipment cost evaluation of the coupled system (SS: stainless steel; CS: carbon steel)

Block name	Equipment type	Material selection	Capacity measure	Equipment size Q	Base size Q_B	C_B (\$)	M	f_M	f_P	f_T	$C_{E,\,2019}$ (\$)
Generator 1	Storage tank	SS	Volume (m^3)	16.72	5	1.15×10^{4}	0.53	2.4	1.3	1.0	1.05×10^{5}
	Shell/tube heat exchanger	SS	Heat transfer area (m^2)	603	80	3.28×10^{4}	0.68	2.9	1.3	1.0	7.53×10^{5}
Condenser	Shell/tube heat exchanger	CS	Heat transfer area (m^2)	880	80	3.28×10^{4}	0.68	1.0	1.3	1.0	3.36×10^{5}
Evaporator	Shell/tube heat exchanger	SS	Heat transfer area (m^2)	307	80	3.28×10^{4}	0.68	2.9	2.0	1.0	7.32×10^{5}
Absorber	Storage tank	SS	Volume (m^3)	16.35	5	1.15×10^{4}	0.53	2.4	2.0	1.0	1.59×10^{5}
Heat exchanger	Shell/tube heat exchanger	SS	Heat transfer area (m^2)	282	80	3.28×10^{4}	0.68	2.9	1.3	1.0	4.49×10^{5}
Pump 1	Centrifugal pump	SS	Power (kW)	0.28	1	1.97×10^{3}	0.35	3.4	2.0	1.0	1.32×10^{4}
Generator 2	Distillation column	SS	Mass (t)	17.85	8	6.56×10^{4}	0.89	2.1	1.5	1.0	6.51×10^{5}
	Sieve trays	SS	Column diameter (m)	1.86	0.5	6.56×10^{3}	0.91	2.4	1.5	1.0	1.20×10^{5}
Turbine	Compressor	SS	Power (kW)	4316	250	9.84×10^{4}	0.46	2.4	1.5	1.0	2.02×10^{6}
Mixer	Storage tank	SS	Volume (m^3)	18.04	5	1.15×10^{4}	0.53	2.4	1.0	1.0	8.40×10^{4}
HT recuperator	Shell/tube heat exchanger	SS	Heat transfer area (m^2)	960	80	3.28×10^{4}	0.68	2.9	1.5	1.0	1.19×10^{6}
LT recuperator	Shell/tube heat exchanger	SS	Heat transfer area (m^2)	183	80	3.28×10^{4}	0.68	2.9	1.5	1.0	3.86×10^{5}
Pump 2	Centrifugal pump	SS	Power (kW)	251	4	9.84×10^{3}	0.55	2.4	1.5	1.0	5.32×10^{5}

which is close to the estimated price \$ 2.02×10^6 in Table 3 (with a relative error of less than 7%). However, the recommended range of W_{turbine} for this correlation equation is from 100 to 4000 kW. While W_{turbine} in this work is obtained as 4316 kW, being slightly higher than the recommended upper limit. Thus, the estimated value in Table 3 is retained for the economic analysis. Except for the equipment delivered price, there are still many other expenses should be considered for the practical operation of the proposed system. The fixed capital cost of the whole system can be calculated as

$$C_{\mathrm{F}} = \sum_i [f_{\mathrm{M}} f_{\mathrm{P}} f_{\mathrm{T}} (1 + f_{\mathrm{pip}})]_i C_{\mathrm{E},i} + (f_{\mathrm{er}} + f_{\mathrm{inst}} + f_{\mathrm{elec}} + f_{\mathrm{util}} + f_{\mathrm{os}} + f_{\mathrm{build}} + f_{\mathrm{sp}} + f_{\mathrm{dec}} + f_{\mathrm{cont}} + f_{\mathrm{ws}}) \sum_i C_{\mathrm{E},i} \tag{63}$$

where i refers to the equipment i; f_{pip} is the correction factor for pipe connection; f_{er} is the correction factor for equipment erection; f_{inst} is the correction factor for instrumentation and controls; f_{elec} is the correction factor for electrical; f_{util} is the correction factor for utilities; f_{os} is the correction factor for off-sites; f_{build} is the correction factor for buildings; f_{sp} is the correction factor for site preparation; f_{dec} is the correction factor for design, engineering and construction; f_{cont} is the correction factor for contingency; f_{ws} is the correction factor for working capital; and C_{F} is the fixed capital cost for the complete system. The specific value of each correction factor and the fixed capital cost for the whole system are given in Table 4. The fixed capital cost is calculated as \$ 2.09×10^7. For a complete economic analysis of this system, some specifications have to be made in advance. Considering the influence of currency devaluation on the system economic performance, the effective discount rate is specified as 5% [51]. The world average electricity price for business users is 0.12 dollar per kWh [52]. To calculate the benefits of this proposed system, the electricity price and operation time per year are currently specified as 0.12 \$/kWh and 8760 h.

Table 4 Correction factors and the fixed capital cost

Item	Value
Equipment delivered cost factor	1.0
Pipe connection, f_{pip}	0.7
Equipment erection, f_{er}	0.4
Instrumentation and controls, f_{inst}	0.2
Electrical, f_{elec}	0.1
Utilities, f_{util}	0.5
Off-sites, f_{os}	0.2
Buildings, f_{build}	0.2
Site preparation, f_{sp}	0.1
Design, engineering and construction, f_{dec}	1.0
Contingency, f_{cont}	0.4
Working capital, f_{ws}	0.7
Fixed capital cost, C_{F} (\$)	2.09×10^7

Payback time, Return on investment (ROI), Net present value (NPV) and discounted cash flow rate of return (DCFRR) are selected as economic indicators in present work for a comprehensive economic analysis of the proposed system. Payback time is the period from the start of the project to the breakeven point. It is calculated by subtracting the accumulated annual income from the capital cost of the project until the balance of payment. ROI is the ratio of annual average income to the capital investment. It is calculated by dividing the annual average value of accumulated income using the capital cost of the project. Payback time and ROI represent the profitability of a project while ignore the effect of time on the system economic performance. NPV is the sum of the present value of individual cash flow and it can be calculated as

$$NPV = \sum_n A_{\mathrm{DCFn}} = \frac{A_{\mathrm{CF1}}}{(1+i)} + \frac{A_{\mathrm{CF2}}}{(1+i)^2} + \frac{A_{\mathrm{CF3}}}{(1+i)^3} + \cdots \frac{A_{\mathrm{CFn}}}{(1+i)^n} \tag{64}$$

where i is the interest rate (effective discount rate); A_{CFn} is the annual cash flow at the end of year n; A_{DCFn} is the annual discounted cash flow at the end of year n. DCFRR can be obtained by solving the Eq. (64). It is the value of discounted interest rate which makes NPV equal zero [48]. The predicted annual cash flow (considering the effect of currency devaluation or not), payback time, ROI, NPV and DCFRR are calculated and then given in Table 5. The calculation is carried out in a short time period of 10 years, for the worst case. The construction of this project is completed at the end of the year 0 and the benefit is realized from the year 1. The income is lowered down to 80 and 50% in the penultimate year 8 and the last year 9 [37]. The discounted interest rate is specified at $i = 0$, $i = 5\%$ and $i = \mathrm{DCFRR}$, respectively. The balance of payment can be achieved in 5 years when the interest rate is zero. In consideration of time value of cash flow, the payback time is 1 year longer but still less than 6 years. The proposed system is more attractive when the payback time is shorter. ROI of these two cases ($i = 0$, $i = 5\%$) are 18.88% and 15.13%, respectively. NPV of this system at $i = 0$ and $i = 5\%$ are calculated as 14.60 and 7.55. These indicators indicate that the coupled system is basically a profitable project even in a short lifetime of 10 years. If the system runs normally for a longer time, more optimistic economic performance would be obtained. By solving the equation NPV = 0, the value of DCFRR is calculated as 13.04%, which means that it will takes more than 10 years to make profit from the project when the discounted interest rate is 13.04% or higher. If the value of DCFRR is lower than the interest rate, it would be safer to put the money in the bank. The cash flow patterns of the proposed system at $i = 0$, $i = 5\%$ and $i = \mathrm{DCFRR}$ are illustrated in Fig. 4a. It can be found that

Table 5 Predicted annual cash flow and economic indicators for different discounted interest rates

Item	Discounted rate					
	$i=0$		$i=5\%$		$i=$DCFRR	
Year	A_{CFn}	$\sum A_{CFn}$	A_{DCFn}	$\sum A_{DCFn}$	A_{DCFn}	$\sum A_{DCFn}$
0	−20.87	−20.87	−20.87	−20.87	−20.87	−20.87
1	4.27	−16.60	4.07	−16.80	3.78	−17.09
2	4.27	−12.32	3.88	−12.92	3.34	−13.74
3	4.27	−8.05	3.69	−9.23	2.96	−10.79
4	4.27	−3.78	3.52	−5.72	2.62	−8.17
5	4.27	0.50	3.35	−2.37	2.32	−5.85
6	4.27	4.77	3.19	0.82	2.05	−3.80
7	4.27	9.04	3.04	3.86	1.81	−1.99
8	3.42	12.46	2.31	6.17	1.28	−0.71
9	2.14	14.60	1.38	7.55	0.71	0
Payback time (year)	5		6		9	
ROI	18.88%		15.13%		11.11%	
NPV	14.60		7.55		0	
DCFRR	/		/		13.04%	

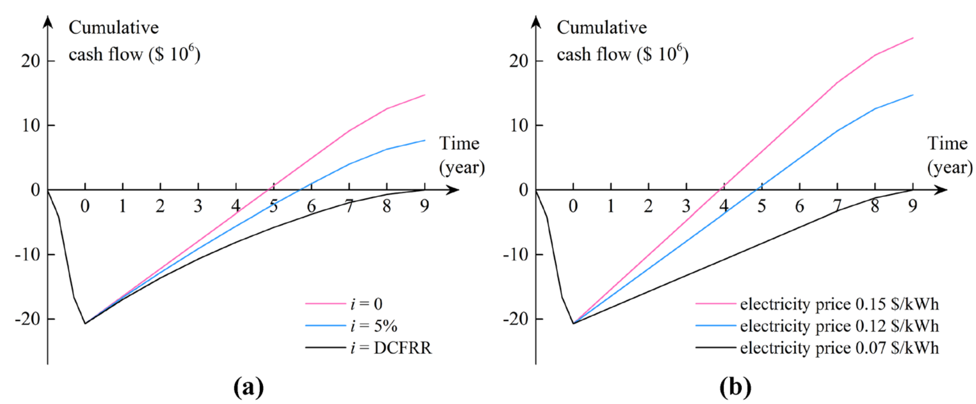

Fig. 4 Cash flow pattern for different interest rates (**a**) and different electricity prices (**b**)

the interest rate has a great influence on the cash flow pattern of the system. The payback time can be shortened for years. The proposed system would be more profitable and more attractive at lower discounted interest rate.

Electricity price decides the utility expenses for the daily operation of a project. Table 6 gives the predicted annual cash flow, payback time, ROI, NPV and DCFRR when the electricity price is fixed at 0.07 $/kWh, 0.12 $/kWh and 0.15 $/kWh, respectively. When the electricity price is 0.07 $/kWh, it would take more than 9 years to achieve the balance of payment. The proposed system would be unprofitable at all in 10 years. Extending the lifetime of this coupled system might be an effective way of improving the economic performance. The economic performance of this system is acceptable when the electricity price is 0.12 $/kWh. If the electricity price is 0.15 $/kWh, the time for balance of payment is predicted to reduce by 5 years. The payment balance can be achieved at the end of year 4. The value of ROI is higher than 20% and DCFRR is around 20% at this case. Therefore, the electricity price is proved to be another critical factor of the economic performance of this system. The cash flow patterns of the proposed system for different electricity prices are illustrated in Fig. 4b. It can also be found that the electricity price has a significant effect on the cash flow pattern of the system. Obviously, the proposed system would be more profitable when the generated electricity is sold at a higher price.

4.3 Exergetic Analysis

Exergy analysis helps to find the reason for the system inefficiency and to quantify the system irreversibility. Exergy analysis has also been conducted for the LiBr/H_2O absorption chiller and the Kalina cycle in this work. Figure 5 depicts the distribution of exergy inflow and exergy loss of these two subcycles and the electrical power production of

Table 6 Predicted annual cash flow and economic indicators for different electricity prices

Item	Electricity price (U.S. dollar per kWh)					
	0.07		0.12		0.15	
Year	A_{CFn}	$\sum A_{CFn}$	A_{CFn}	$\sum A_{CFn}$	A_{CFn}	$\sum A_{CFn}$
0	−20.87	−20.87	−20.87	−20.87	−20.87	−20.87
1	2.50	−18.37	4.27	−16.60	5.34	−15.53
2	2.50	−15.88	4.27	−12.32	5.34	−10.19
3	2.50	−13.38	4.27	−8.05	5.34	−4.85
4	2.50	−10.89	4.27	−3.78	5.34	0.50
5	2.50	−8.39	4.27	0.50	5.34	5.84
6	2.50	−5.89	4.27	4.77	5.34	11.18
7	2.50	−3.40	4.27	9.04	5.34	16.52
8	2.00	−1.40	3.42	12.46	4.27	20.79
9	1.25	−0.15	2.14	14.60	2.67	23.46
Payback time (year)	9+		5		4	
ROI	11.03%		18.88%		23.77%	
NPV	−0.15		14.60		23.60	
DCFRR	/		13.04%		19.84%	

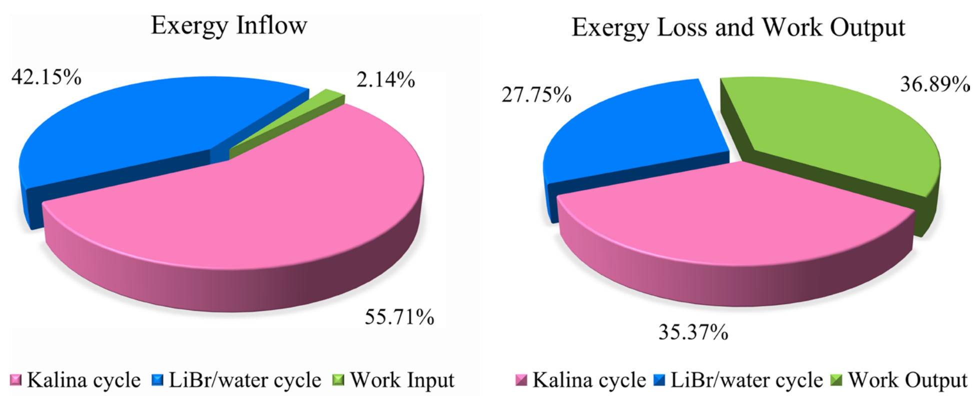

Fig. 5 Distribution of exergy input, exergy loss and electrical power output

the coupled cycle. It can be seen in this figure that more than a half of the exergy in the wasted thermal energy is for electricity generation in the Kalina cycle. Only 42.15% of the exergy input is recovered by the absorption refrigeration system for cooling output. Around 2% of the exergy inflow is the work input of pumps for liquid pumping. The total exergy loss of this couple system occupies more than 60% of the total exergy input. It indicates that more than 60% of the exergy is lost in this coupled system hence the exergy efficiency of this system is 36.89%. The electrical power output of this system is 4065 kW. The exergy loss in the Kalina cycle is more significant than that in the LiBr/H_2O absorption chiller. This can be explained as the higher temperature of working stream as well as the larger temperature difference in the Kalina power generation cycle than those in the absorption refrigeration cycle.

Exergy loss of each component in both cycles has also been obtained and then illustrated in details in Fig. 6. In the LiBr/H_2O absorption chiller, the largest exergy loss is in the generator (Generator 1) and the value is 1149.12 kW (35.41% of the total exergy loss). Condenser, Absorber and Heat exchanger occupy the 22.88, 20.76 and 17.70% of the total loss, respectively. Less than 4% of the total exergy loss in the absorption refrigeration system is found in Valve 1, Evaporator (cold side), Pump 1 and Valve 2. The exergy loss at the cold side of the evaporator is insignificant, because the flow rate of the refrigerant water is small. In the Kalina cycle, the total exergy loss is larger and a more concentrated distribution can be noticed. The exergy lost in Generator 2 occupies a larger proportion (44.02% of the total) than that of Generator 1. The second to the fourth largest exergy loss of the Kalina cycle is in high-temperature recuperator, Evaporator (hot side) and Turbine, with proportions of 17.52%, 17.24 and 15.43% of the total value. The exergy loss at the hot side of the evaporator is more significant than that at the cold side,

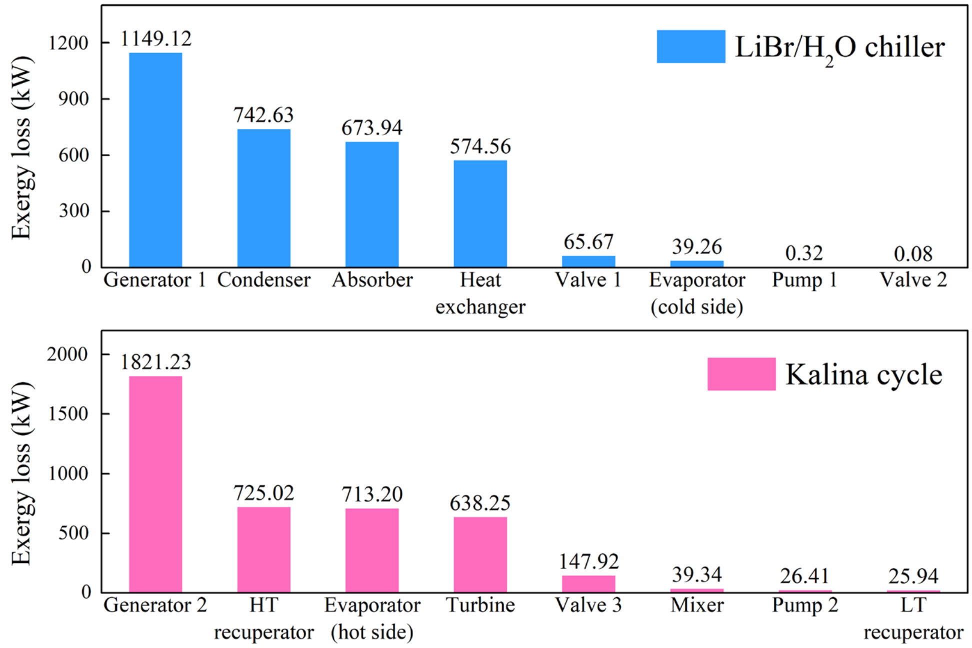

Fig. 6 Exergy loss distribution of both subcycles

because the temperature difference of the hot side is 10 °C, higher than that of the cold side. Besides, the flow rate of the ammonia solution is larger than the flow rate of water at the cold side. Less than 6% of the total exergy loss in the power generation system is found in Valve 3, Mixer, Pump 2 and low-temperature recuperator. The heat exchange processes in high- and low-temperature recuperators are sensible heat transfer processes. The exergy loss in high-temperature recuperator is more significant than that in low-temperature recuperator. It is because the calculated heat duty in high-temperature recuperator is much larger than that in low-temperature recuperator. Besides, the logarithmic mean temperature difference (LMTD) in the high-temperature recuperator is around 16 °C, being higher than the value 7 °C of low-temperature recuperator. It can also be concluded in this figure that the most significant exergy loss is in heat transfer processes in these heat exchangers. Therefore, reducing the irreversibility in the heat transfer processes will be greatly encouraged in future efforts.

5 Conclusions

A $LiBr/H_2O$ absorption refrigeration cycle and a Kalina cycle are integrated to utilize the low-grade waste heat in a cascade approach. The mathematical models for this coupled system have been established. This coupled system is investigated to achieve its optimal operation. Then, it is employed to recover the wasted heat from a two-stage hydrate-based CO_2 capture process. Economic analysis and exergy analysis of the proposed system have been carried out. Payback time, Return on investment, Net present value and Discounted cash flow rate of return are selected as major indicators for a comprehensive economic analysis. Cash flow patterns of this system have been obtained for different discounted interest rates and electricity prices. Exergy loss of all the components and the overall exergy efficiency has also been obtained.

The proposed system reaches to a lower turbine discharge pressure when the refrigeration temperature is fixed. Among all the studied cases, the highest thermal efficiency is obtained as 16.78%. With the help of the absorption chiller, the net power output is improved by around 45%. In the economic analysis, the purchase price of heat exchanger occupies the largest capital investment. The payback time of this integrated system is less than 6 years. The proposed system would be more profitable and more attractive at lower discounted interest rate and higher electricity price. Exergy analysis results show that the major system irreversibility is in heat transfer processes of heat exchangers and the overall exergy efficiency is 36.89%. The largest exergy loss is found in generators in both cycles. The exergy loss in the Kalina cycle is more significant than that in the absorption chiller because the higher temperature of working stream and larger heat transfer temperature difference. Therefore, reducing the inefficiency in heat transfer processes and the size of heat exchangers is the most effective way to improve the system performance. Economic and exergy analysis in this research will be useful for future application of the absorption chiller/Kalina cycle-coupled system and the energy penalty reduction in the hydrate-based CO_2 capture process.

Authors' Contributions ZL was responsible for the funding acquisition, resources and supervision of the study. KW carried out the methodology section of this research. NX carried out the conceptualization, formal analysis and investigation, original draft preparation, review and editing of the manuscript. All authors read and approved the final manuscript.

Funding This work was supported by [the National Natural Science Foundation of China] (Grant number [51676209] and [22008265]).

Availability of Data and Materials The data sets generated during and/or analysed during the current study are available from the corresponding author on reasonable request.

Declarations

Conflict of Interest The authors have no relevant financial or non-financial interests to disclose.

Ethics Approval and Consent to Participate Not applicable.

Consent for Publication Not applicable.

References

1. Zhang, X., He, M., Zhang, Y.: A review of research on the Kalina cycle. Renew. Sustain. Energy Rev. **16**, 5309–5318 (2012)
2. Wang, J., Yan, Z., Zhou, E., Dai, Y.: Parametric analysis and optimization of a Kalina cycle driven by solar energy. Appl. Therm. Eng. **50**, 408–415 (2013)
3. Júnior, E.P.B., Arrieta, M.D.P., Arrieta, F.R.P., Silva, C.H.F.: Assessment of a Kalina cycle for waste heat recovery in the cement industry. Appl. Therm. Eng. **147**, 421–437 (2019)
4. Singh, O.K., Kaushik, S.C.: Energy and exergy analysis and optimization of Kalina cycle coupled with a coal fired steam power plant. Appl. Therm. Eng. **51**, 787–800 (2013)
5. He, J., Liu, C., Xu, X., Li, Y., Wu, S., Xu, J.: Performance research on modified KCS (Kalina cycle system) 11 without throttle valve. Energy **64**, 389–397 (2014)
6. Li, H., Hu, D., Wang, M., Dai, Y.: Off-design performance analysis of Kalina cycle for low temperature geothermal source. Appl. Therm. Eng. **107**, 728–737 (2016)
7. Zhang, L., Pan, Z., Zhang, Z., Shang, L., Wen, J., Chen, S.: Thermodynamic and economic analysis between organic Rankine cycle and Kalina cycle for waste heat recovery from steam-assisted gravity drainage process in oilfield. J. Energy Resour. Technol. **140**, 122005 (2018)
8. Ochoa, A.A.V., Dutra, J.C.C., Henríquez, J.R.G., dos Santos, C.A.C., Rohatgi, J.: The influence of the overall heat transfer coefficients in the dynamic behavior of a single effect absorption chiller using the pair LiBr/H_2O. Energy Convers. Manage. **136**, 270–282 (2017)
9. Heng, Z., Feipeng, C., Yang, L., Haiping, C., Kai, L., Boran, Y.: The performance analysis of a LCPV/T assisted absorption refrigeration system. Renew. Energy **143**, 1852–1864 (2019)
10. Pandya, B., Patel, J., Mudgal, A.: Thermodynamic evaluation of generator temperature in LiBr water absorption system for optimal performance. Energy Procedia **109**, 270–278 (2017)
11. Lamine, C.M., Said, Z.: Energy analysis of single effect absorption chiller (LiBr/H_2O) in an industrial manufacturing of detergent. Energy Procedia **50**, 105–112 (2014)
12. Wang, R.Z., Xu, Z.Y., Pan, Q.W., Du, S., Xia, Z.Z.: Solar driven air conditioning and refrigeration systems corresponding to various heating source temperatures. Appl. Energy **169**, 846–856 (2016)
13. Lee, S.K., Lee, J.W., Lee, H., Chung, J.T., Kang, Y.T.: Optimal design of generators for H_2O/LiBr absorption chiller with multi-heat sources. Energy **167**, 47–59 (2019)
14. Mohammadi, S.M.H., Ameri, M.: Energy and exergy performance comparison of different configurations of an absorption-two-stage compression cascade refrigeration system with carbon dioxide refrigerant. Appl. Therm. Eng. **104**, 104–120 (2016)
15. Razmi, A., Soltani, M., Kashkooli, F.M., Garousi Farshi, L.: Energy and exergy analysis of an environmentally-friendly hybrid absorption/recompression refrigeration system. Energy Convers. Manag. **164**, 59–69 (2018)
16. Mohammadi, S.M.H.: Theoretical investigation on performance improvement of a low-temperature transcritical carbon dioxide compression refrigeration system by means of an absorption chiller after-cooler. Appl. Therm. Eng. **138**, 264–279 (2018)
17. Rosiek, S.: Exergy analysis of a solar-assisted air-conditioning system: case study in southern Spain. Appl. Therm. Eng. **148**, 806–816 (2019)
18. Cao, L., Wang, J., Wang, H., Zhao, P., Dai, Y.: Thermodynamic analysis of a Kalina-based combined cooling and power cycle driven by low-grade heat source. Appl. Therm. Eng. **111**, 8–19 (2017)
19. Akbari Kordlar, M., Mahmoudi, S.M.S., Talati, F., Yari, M., Mosaffa, A.H.: A new flexible geothermal based cogeneration system producing power and refrigeration, part two: the influence of ambient temperature. Renew. Energy **134**, 875–887 (2019)
20. Wang, J., Wang, J., Zhao, P., Dai, Y.: Thermodynamic analysis of a new combined cooling and power system using ammonia–water mixture. Energy Convers. Manage. **117**, 335–342 (2016)
21. Shokati, N., Ranjbar, F., Yari, M.: A comprehensive exergoeconomic analysis of absorption power and cooling cogeneration cycles based on Kalina, part 1: Simulation. Energy Convers. Manage. **158**, 437–459 (2018)
22. Shokati, N., Ranjbar, F., Yari, M.: A comprehensive exergoeconomic analysis of absorption power and cooling cogeneration cycles based on Kalina, Part 2: Parametric study and optimization. Energy Convers. Manage. **161**, 74–103 (2018)
23. Rashidi, J., Yoo, C.K.: Exergetic and exergoeconomic studies of two highly efficient power-cooling cogeneration systems based on the Kalina and absorption refrigeration cycles. Appl. Therm. Eng. **124**, 1023–1037 (2017)
24. Rashidi, J., Ifaei, P., Esfahani, I.J., Ataei, A., Yoo, C.K.: Thermodynamic and economic studies of two new high efficient power-cooling cogeneration systems based on Kalina and absorption refrigeration cycles. Energy Convers. Manage. **127**, 170–186 (2016)

25. Qu, W., Su, B., Tang, S., Hong, H.: Thermodynamic Evaluation of a hybrid solar concentrating photovoltaic/Kalina cycle for full spectrum utilization. Energy Procedia **142**, 597–602 (2017)
26. Qu, W., Hong, H., Su, B., Tang, S., Jin, H.: A concentrating photovoltaic/Kalina cycle coupled with absorption chiller. Appl. Energy **224**, 481–493 (2018)
27. Liu, Z., Xie, N., Yang, S.: Thermodynamic and parametric analysis of a coupled LiBr/H_2O absorption chiller/Kalina cycle for cascade utilization of low-grade waste heat. Energy Convers. Manage. **205**, 112370 (2020)
28. Dashti, H., Zhehao Yew, L., Lou, X.: Recent advances in gas hydrate-based CO_2 capture. J. Nat. Gas Sci. Eng. **23**, 195–207 (2015)
29. Giavarini, C., Maccioni, F., Santarelli, M.L.: CO_2 sequestration from coal fired power plants. Fuel **89**, 623–628 (2010)
30. Delahaye, A., Fournaison, L., Marinhas, S., Chatti, I., Petitet, J.-P., Dalmazzone, D., Fürst, W.: Effect of THF on equilibrium pressure and dissociation enthalpy of CO_2 hydrates applied to secondary refrigeration. Ind. Eng. Chem. Res. **45**, 391–397 (2006)
31. Xie, N., Chen, B., Tan, C., Liu, Z.: Energy consumption and exergy analysis of MEA-based and hydrate-based CO_2 separation. Ind. Eng. Chem. Res. **56**, 15094–15101 (2017)
32. Ma, Z.W., Zhang, P., Bao, H.S., Deng, S.: Review of fundamental properties of CO_2 hydrates and CO_2 capture and separation using hydration method. Renew. Sustain. Energy Rev. **53**, 1273–1302 (2016)
33. Sadeq, D., Iglauer, S., Lebedev, M., Smith, C., Barifcani, A.: Experimental determination of hydrate phase equilibrium for different gas mixtures containing methane, carbon dioxide and nitrogen with motor current measurements. J. Nat. Gas Sci. Eng. **38**, 59–73 (2017)
34. Smith, C., Barifcani, A., Pack, D.: Gas hydrate formation and dissociation numerical modelling with nitrogen and carbon dioxide. J. Nat. Gas Sci. Eng. **27**, 1118–1128 (2015)
35. Zhong, D.-L., Wang, Y.-R., Lu, Y.-Y., Wang, W.-C., Wang, J.-L.: Phase equilibrium and kinetics of gas hydrates formed from CO_2/H_2 in the presence of tetrahydrofuran and cyclohexane. J. Nat. Gas Sci. Eng. **35**, 1566–1572 (2016)
36. Pan, Z., Zhang, L., Zhang, Z., Shang, L., Chen, S.: Thermodynamic analysis of KCS/ORC integrated power generation system with LNG cold energy exploitation and CO_2 capture. J. Nat. Gas Sci. Eng. **46**, 188–198 (2017)
37. Yang, S., Qian, Y., Wang, Y., Yang, S.: A novel cascade absorption heat transformer process using low grade waste heat and its application to coal to synthetic natural gas. Appl. Energy **202**, 42–52 (2017)
38. Yang, S., Wang, Y., Gao, J., Zhang, Z., Liu, Z., Olabi, A.G.: Performance analysis of a novel cascade absorption refrigeration for low-grade waste heat recovery. ACS Sustain. Chemi. Eng. **6**, 8350–8363 (2018)
39. Yang, S., Yang, S., Wang, Y., Qian, Y.: Low grade waste heat recovery with a novel cascade absorption heat transformer. Energy **130**, 461–472 (2017)
40. Jing, X., Zheng, D.: Effect of cycle coupling-configuration on energy cascade utilization for a new power and cooling cogeneration cycle. Energy Convers. Manage. **78**, 58–64 (2014)
41. Seckin, C.: Thermodynamic analysis of a combined power/refrigeration cycle: Combination of Kalina cycle and ejector refrigeration cycle. Energy Convers. Manage. **157**, 631–643 (2018)
42. Xu, C.-G., Chen, Z.-Y., Cai, J., Li, X.-S.: Study on pilot-scale CO_2 separation from flue gas by the hydrate method. Energy Fuels **28**, 1242–1248 (2013)
43. Meysel, P., Oellrich, L., Raj Bishnoi, P., Clarke, M.A.: Experimental investigation of incipient equilibrium conditions for the formation of semi-clathrate hydrates from quaternary mixtures of (CO_2+N_2+TBAB+H_2O). J. Chem. Thermodyn. **43**, 1475–1479 (2011)
44. Arjmandi, M., Chapoy, A., Tohidi, B.: Equilibrium data of hydrogen, methane, nitrogen, carbon dioxide, and natural gas in semi-clathrate hydrates of tetrabutyl ammonium bromide. J. Chem. Eng. Data **52**, 2153–2158 (2007)
45. Lin, W., Delahaye, A., Fournaison, L.: Phase equilibrium and dissociation enthalpy for semi-clathrate hydrate of CO_2+TBAB. Fluid Phase Equilib. **264**, 220–227 (2008)
46. Li, Z., Zhong, D.-L., Lu, Y.-Y., Wang, J.-L., Qing, S.-L., Yan, J.: Enhanced separation of carbon dioxide from a $CO_2 + CH_4$ gas mixture using a hybrid adsorption-hydrate formation process in the presence of coal particles. J. Nat. Gas Sci. Eng. **35**, 1472–1479 (2016)
47. Fan, S., Li, S., Wang, J., Lang, X., Wang, Y.: Efficient capture of CO_2 from simulated flue gas by formation of TBAB or TBAF semiclathrate hydrates. Energy Fuels **23**, 4202–4208 (2009)
48. Smith, R.: Chemical Process Design and Integration, 2nd edn. Wiley, Chichester (2016)
49. CHEMICAL ENGINEERING PLANT COST INDEX: 2018 ANNUAL VALUE, in, 2019. URL: https://www.chemengonline.com/2019-cepci-updates-january-prelim-and-december-2018-final/
50. Turton, R., Bailie, R.C., Whiting, W.B., Shaeiwitz, J.A., Bhattacharyya, D.: Analysis, Synthesis, and Design of Chemical Processes. Pearson Education, Upper Saddle River (2008)
51. Ipakchi, O., Mosaffa, A.H., Garousifarshi, L.: Ejector based CO_2 transcritical combined cooling and power system utilizing waste heat recovery: A thermoeconomic assessment. Energy Convers. Manag. **186**, 462–472 (2019)
52. Electricity prices around the world, March 2019, in, 2019. URL: https://www.globalpetrolprices.com/electricity_prices/